

Chapter 3

Dealloying Toxic Ni from SUS316L Surface

Hidemi Kato, Takeshi Wada, and Sadeghilaridjani Maryam

Abstract SUS316L (18 %Cr-12 %Ni-2.5 %Mo-<0.03 %C) is one of the most popular metallic materials for biomedical uses such as implants and surgical instruments owing to its lower cost, good corrosion resistance, and excellent workability compared with those of other types of biomedical metallic materials. Although Ni stabilizes the austenitic FCC structure to give the excellent workability of SUS316L, elution of toxic Ni ions into the human body can cause various health problems. In SUS316L, the elution of Ni ions is suppressed by the stable passive thin film arising from the Cr component. However, there remains some risk of Ni elution. In this paper, we remove Ni element from the surface of SUS316L using a novel dealloying technique with a metallic melt and study its effect on the corrosion resistance and Ni ion elution of the steel in a simulated human body fluid.

Keywords SUS316L • Biomedical material • Ni • Dealloying • Surface improvement

3.1 Introduction

SUS316L (18 % Cr, 12 % Ni, 2.5 % Mo, <0.03 %C) is an austenitic stainless steel that contains 18 wt% Cr, 12 wt% Ni, 2.5 % Mo, and less than 0.03 % C (the “L” in 316L standing for low carbon), which tends to degrade the stability of the face-centered cubic (FCC) structure and segregate as carbides in grain boundaries, causing intergranular cracking. Owing to these elements, SUS316L has the advantages of high corrosion resistance, excellent workability, low cost, and highly reliable mechanical properties and has thus been widely used as a biomedical material, such as in surgical instruments and bone fixtures. The Ni element in SUS316L stabilizes

H. Kato (✉) • T. Wada
Institute for Materials Research, Tohoku University,
2-1-1 Katahira, Aoba-ku, Sendai, Miyagi 980-8577, Japan
e-mail: hikato@imr.tohoku.ac.jp

S. Maryam
Department of Materials Science, Tohoku University, Sendai, Miyagi, Japan

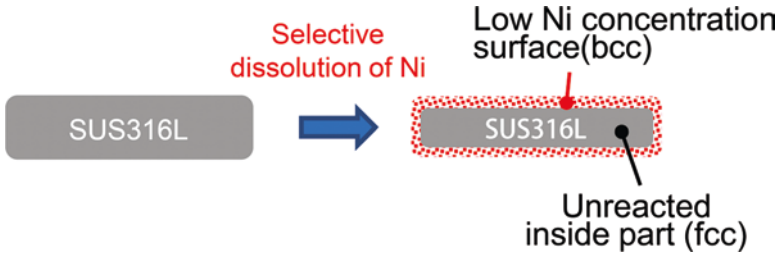


Fig. 3.1 Strategy of the present research for improving the biocompatibility of SUS316L

the FCC structure to produce excellent workability. However, Ni is a toxic element, meaning that using SUS316L potentially risks causing health problems. Therefore, Ni is necessary for workability but is unwanted for the biocompatibility of SUS316L. To solve this problem, we investigated the removal of Ni element from the surface of SUS316L using a novel dealloying technique, “dealloying in metallic melt,” as shown in Fig. 3.1. This work intends to demonstrate the dealloying of Ni element from the SUS316L surface and investigate its effects on the corrosion resistance and Ni ion release of the SUS316L in Hank’s balanced salt solution (HBSS).

3.1.1 Dealloying in a Metallic Melt

This method is first reported in Ref. [1], and its principle was mentioned in Ref. [2] as follows. When two metal elements are mixed, the free energy change is

$$\Delta G_{mix} = \Delta H_{mix} - T \Delta S_{mix}, \quad (3.1)$$

where ΔH_{mix} is the heat of mixing, ΔS_{mix} is the entropy of mixing, and T is the absolute temperature. Usually, the entropy increases after mixing. Therefore, if $\Delta H_{mix} < 0$, then $\Delta G_{mix} < 0$, and the mixing reaction can occur spontaneously from a thermodynamic point of view. Conversely, if $\Delta H_{mix} > 0$, the sign (positive or negative) of ΔG_{mix} depends on the temperature. If the temperature is adequately controlled to make the enthalpy term larger than the entropy term, then $\Delta G_{mix} > 0$, and the mixture of the two elements is prevented. Here, we dip an A–B binary alloy precursor into a metallic melt consisting of element C. If the heat of mixing between elements B and C is negative, i.e., $\Delta H_{mix,B-C} < 0$ and if the heat of mixing between elements A and C is positive, i.e., $\Delta H_{mix,A-C} > 0$, then by adequately controlling the temperature, only element B will dissolve from the precursor into the C melt. Because in this case element A is rejected from the C melt, it is expected to self-organize into a porous structure by surface diffusion in the same manner as that of the ordinary dealloying method in aqueous solution [3, 4]. Figure 3.2 shows a schematic of this novel dealloying method involving the selective dissolution of B atoms (orange) in the C atom melt (pink) and surface diffusion of the remaining A atoms

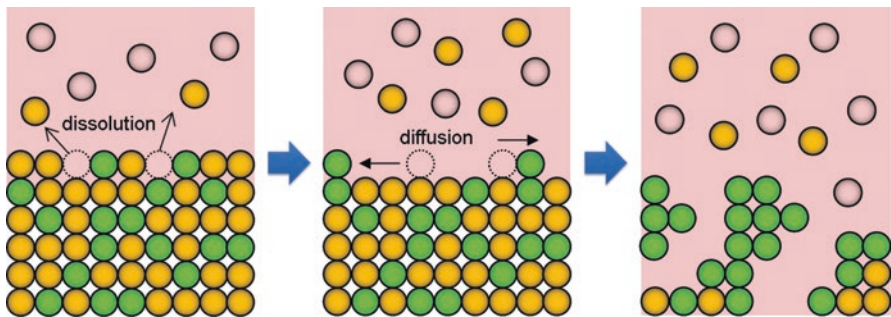
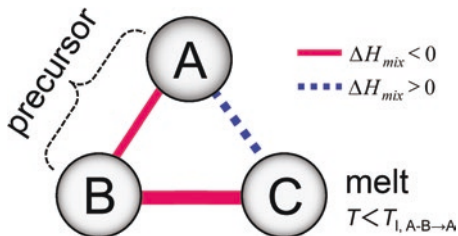


Fig. 3.2 Schematic of the dealloying method using a metallic melt, in which B atoms (orange) dissolve into a melt composed of C atoms (pink), and the remaining A atoms (yellowish green) self-organizes into a porous structure by surface diffusion [3]

Fig. 3.3 Triangle relationship of the enthalpies of mixing among elements A, B, and C for dealloying in a metallic melt [1]

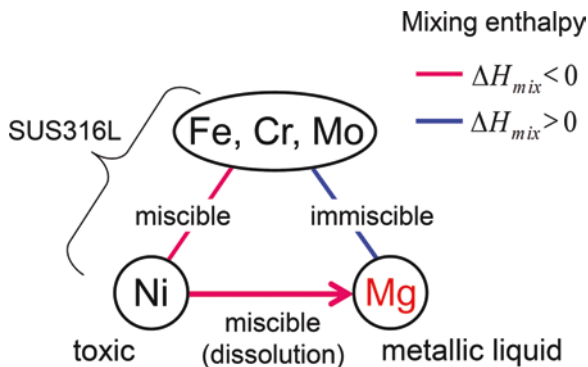


(yellowish green). Figure 3.3 summarizes this “triangle” relationship in terms of the heat of mixing among elements A, B, and C required for the dealloying reaction in a metallic melt. Because the heat of mixing is usually expressed using temperature and chemical composition, we must calculate a rigid value for the heat of mixing with these parameters to design the dealloying reaction. However, this can be complicated. The heat of mixing between the transition metals and between the transition metals and metalloids can be obtained from the table in Ref. [5], the values of which were approximately calculated by the Miedema model, while that of other metals can be obtained from the table constructed by Takeuchi et al. In this study, we first identified the candidates for elements A, B, and C from these values and then confirmed the relationships A–B, B–C (mixture), and A–C (separation) using the related binary phase diagrams if they were available in relevant databases.

3.1.2 Reaction Design for Dealloying Ni from SUS316L

SUS316L consists of Fe, Cr, Mo, and Ni. Mg is miscible with Ni but immiscible with the other elements, which can be confirmed from the corresponding mixing enthalpies: $\Delta H_{\text{mix}} = -4$ kJ/mol (Ni-Mg), +18 kJ/mol (Fe-Mg), +24 kJ/mol (Cr-Mg), and +36 kJ/mol (Mo-Mg) [5]. Thus, as shown in Fig. 3.4, Fe, Cr, and Mo are

Fig. 3.4 Reaction design for removing Ni element from the surface of SUS316L by dealloying in a metallic melt. Here, the carbon component is ignored owing to its low concentration. Based on the mixing enthalpy between each component, Fe, Cr, Mo=A, Ni=B and Mg=C group in Fig. 3.3



regarded as “A” group elements in the triangle relationship in Fig. 3.3, Ni is regarded as a “B” group element, and Mg is regarded as a “C” group element. Therefore, if the temperature is adequately controlled, we can expect that only Ni will dissolve from the surface when SUS316L is dipped into liquid Mg, resulting in the construction of a Fe-Cr-Mo porous alloy in the Mg melt.

3.2 Experimental Procedure

The method used for sample preparation is schematically illustrated in Fig. 3.5. The SUS316L used in this research was a commercial product purchased from Nilaco, Japan, in the form of rods of 10 mm in diameter. The rods were sliced into disks of 1 mm thickness, and these were then cold rolled to ~200 μm thickness. Mg was inductively melted in a chamber under inert argon gas using a graphite crucible.

The temperature of the Mg liquid bath was set to 700 or 900 $^{\circ}\text{C}$, and the cold rolled SUS316L was dipped for 30 min. The resulting dealloyed sample was then dipped in an aqueous solution of HNO_3 to etch away the surrounding Mg-Ni phase, followed by washing and drying. The treated samples were evaluated using scanning electron microscopy-energy dispersive X-ray analysis (SEM-EDX).

Polarization tests were conducted in HBSS solution with a potentiostat/galvanostat (HZ5000, Hokuto Denko, Japan) within a voltage range of -800 to 500 mV vs the Ag/AgCl reference electrode. A pure platinum electrode was used as a counter electrode.

The ion release test was conducted in 1.7 g of HBSS solution at 310 K for 10 days, after which the amount of ions released was evaluated. The HBSS was then replaced with the same weight of fresh solution, and the test was continued for another 14 days. The ion release of Fe, Cr, and Ni was analyzed by inductively coupled plasma optical emission spectrometry (ICP-OES), the detection limit of which was ~ 0.1 μg .

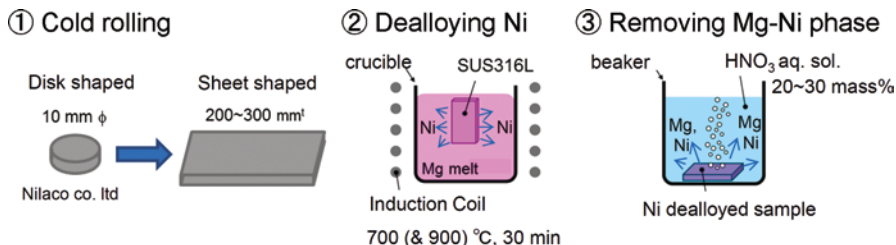


Fig. 3.5 Method for SUS316L surface improvement, i.e., removing toxic Ni from the surface

3.3 Results and Discussion

3.3.1 Dealloying Ni Treatments

The surface and cross section of the samples were observed by SEM, and analysis of their composition was performed by EDX. Cross sections were made by cutting and polishing the samples as shown in Fig. 3.6.

Figure 3.7 shows an SEM image of the surface of a sample that was dealloyed in the Mg melt at 900 °C, the highest temperature in the present study, for 30 min. Hollows and pits are clearly observable, especially in the grain boundaries. It was also found that the characteristic porous structure usually observed on dealloyed surfaces did not develop. The cross-sectional SEM images shown in Fig. 3.8a, b indicate that the sample became thinner, from 200 to ~175 μm , after the dealloying treatment at 900 °C. The composition at point A shown in Fig. 3.8b determined by EDX was $\text{Fe}_{69.4}\text{Cr}_{18.0}\text{Ni}_{11.5}\text{Mo}_{1.1}$ (at. %), which is almost the same as that of the original SUS316L. The homogeneity of the elemental mappings shown in Fig. 3.9a–d indicated that there was no change in the composition of the SUS316L sample after it was dipped into the Mg melt at 900 °C.

Based on these results, i.e., the sample became thinner while keeping its original composition homogeneously, it can be concluded that all the components, Fe, Cr, Ni, and Mo, dissolved from the surface into the Mg melt because its temperature was too high, such that $\Delta G_{\text{mix}} < 0$ in Eq. 3.1. Thus, the temperature of the Mg melt should be lower than 900 °C to prevent the dissolution of the Fe, Cr, and Mo elements in the Mg melt.

Figure 3.10 shows SEM images of the surface (a) and polished cross section (b) and (c) of SUS316L dipped in the Mg melt at 700 °C for 30 min, followed by etching of the surrounding Mg-Ni phase in aqueous HNO₃ solution. The treated surface appeared to be rougher than the pristine sample, and the grain boundaries, which were observed in Fig. 3.7, could no longer be observed. The thickness of this sample was not greatly changed by the dealloying treatment, as shown in Fig. 3.10b. The polished cross section exhibited porous reaction layers of approximately 50 μm in thickness (Fig. 3.10c, similar to that typically observed on traditionally dealloyed sample surfaces [1, 6–9]. Figure 3.11a–d shows the elemental mappings for Fe, Ni,

Fig. 3.6 Cutting direction used to make cross sections for SEM observation and EDX analysis

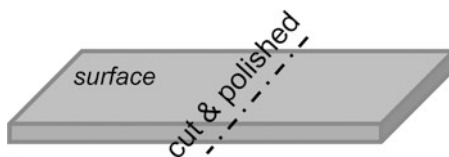


Fig. 3.7 SEM image of the surface of SUS316L sample which was dipped into a Mg melt at 900 °C (highest temperature of the present research) for 30 min, then in aqueous HNO₃ solution to etch away the surrounding Mg-Ni phase

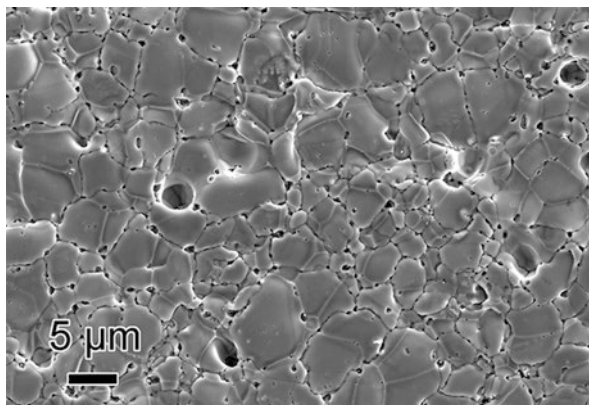
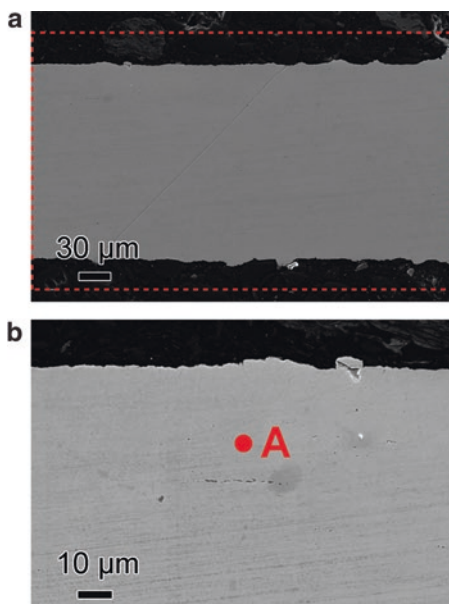


Fig. 3.8 SEM images of (a), (b) polished cross section of SUS316L dealloyed in Mg melt at 900 °C for 30 min. Red dotted line in (a) indicates the initial dimensions of the cross section before the dealloying treatment. Red dot marked A in (b) is the point at which quantitative EDX analysis was conducted



Cr, and Mo of the sample dealloyed in 700 °C for 30 min, respectively. In the Fe, Cr, and Mo mappings, the porous reaction layer was a little brighter than the unreacted part, while that of Ni was clearly darker. This means that the Fe, Cr, and Mo concentrations were a little higher in the reaction layer, while the Ni concentration was

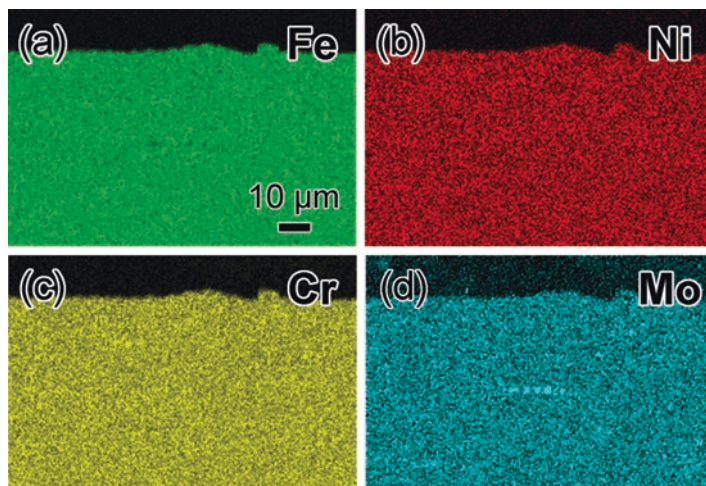


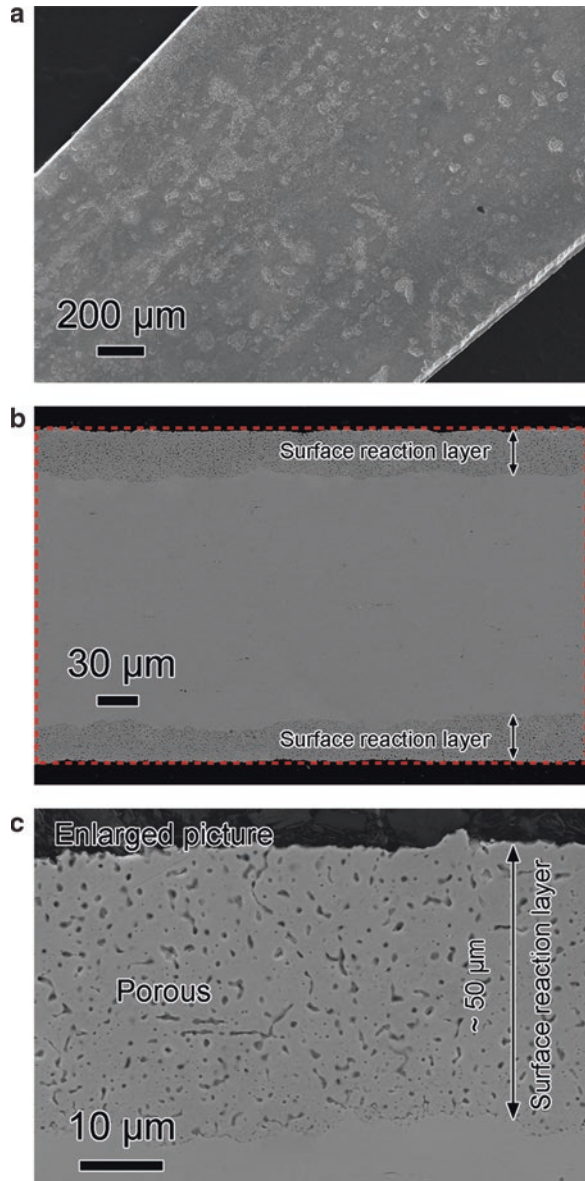
Fig. 3.9 Element mappings for Fe (a), Cr (b), Ni (c), and Mo (d) for the polished cross section of SUS316L dealloyed in Mg melt at 900 °C for 30 min

much lower than in the untreated part. Quantitative analysis of point A in the reacted porous region and point B in the solid inner revealed respective compositions of $\text{Fe}_{76.4}\text{Cr}_{20.0}\text{Ni}_{2.2}\text{Mo}_{1.4}$ (at. %) and $\text{Fe}_{68.9}\text{Cr}_{18.1}\text{Ni}_{11.8}\text{Mo}_{1.2}$ (at.%). The Ni concentration at point A point decreased to 2.2 at.%, which is less than 19% of that at B point in the nonreacted inside. These results indicate that in the Mg melt at 700 °C, almost only the Ni element was removed from the SUS316L by a dealloying reaction, leaving a constricted porous structure.

3.3.2 Polarization Tests

Figure 3.12 shows the polarization curve of the SUS316L dealloyed at 700 °C for 30 min compared with that of the original SUS316L after cold rolling. After the dealloying, the corrosion potential of the SUS316L decreased from -240 to -400 mV, indicating that the dealloying treatment increased the corrodibility of the sample. However, after the corrosion potential, the passive region was maintained up until almost the same potential as that of the original sample. Therefore, it was concluded that the excellent corrosion resistance of the SUS316L was not degraded by the dealloying treatment.

Fig. 3.10 SEM image of surface (a), polished cross section of SUS316L dealloyed in a Mg melt at 700 °C for 30 min (b), and enlarged image of the reacted surface part (c). Red dotted line in (b) indicates the initial dimensions of the cross section before the dealloying treatment



3.3.3 Ion Release Tests

For ion release tests, the original and dealloyed samples were dipped in 1.7 g of HBSS at 37 °C for 10 days, after which the HBSS was replaced with fresh solution and the immersion was continued for another 14 days. Herein, HBSS without samples was used as a reference. The observed ion release of Fe, Cr, and Ni is

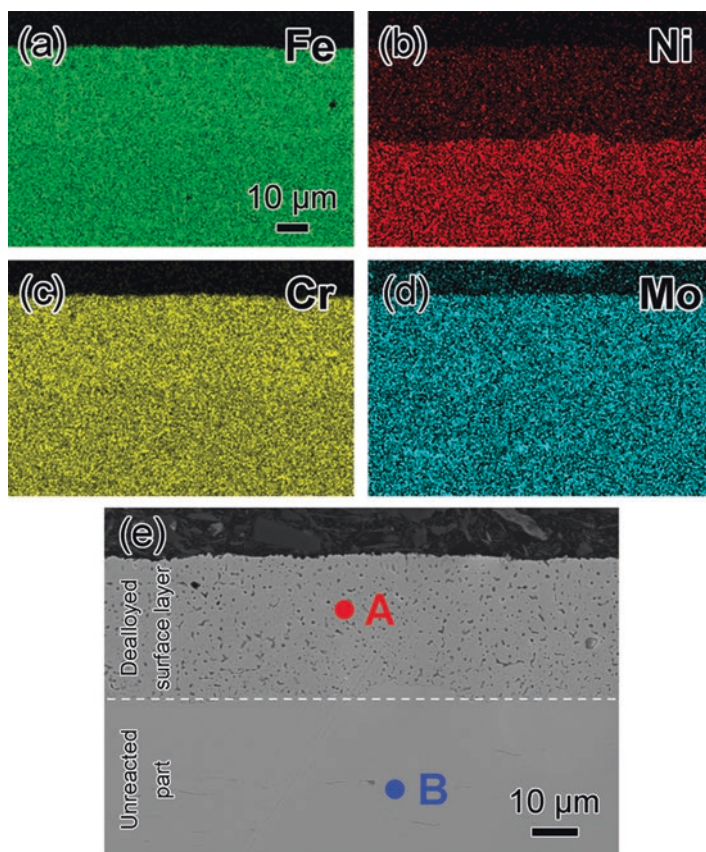


Fig. 3.11 Elemental mappings for Fe (a), Ni (b), Cr (c), and Mo (d) for the polished cross section of SUS316L dealloyed in Mg melt at 700 °C for 30 min, and SEM image taken near the boundary of the dealloyed and unreacted regions (e). Red and blue dots marked A and B in the reacted region and unreacted region, respectively, in (e) are the points at which quantitative EDX analysis was conducted

summarized in Fig. 3.13. During the first 10 days, the Fe ion release from both the original and dealloyed samples was comparatively large, but then decreased over the next 10–24 days. Little Cr release was observed, just within the detection limit, because surface Cr is considered to construct a passivated Cr hydroxide thin film on SUS316L. Ni ion release from the dealloyed sample, which is the most important for us to control, was found to be slightly increased compared with that of the original sample, especially during days 10–24. However, it then decreased after 24 days.

The main reasons for the increased Ni ion release were:

When the Ni in the SUS316L was dealloyed in the Mg melt, a Mg-Ni phase solidified on the surface. This Mg-Ni phase should have been etched away completely in the aqueous HNO₃ solution. However, if Mg-Ni remained after this etching

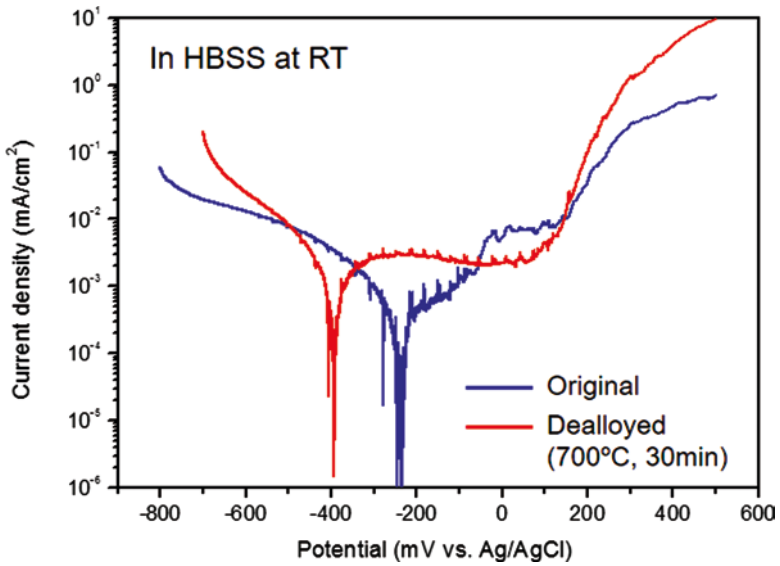


Fig. 3.12 Polarization curves for SUS316L dealloyed in Mg melt at 700 °C for 30 min (*red*) and original SUS316L after cold rolling (*blue*)

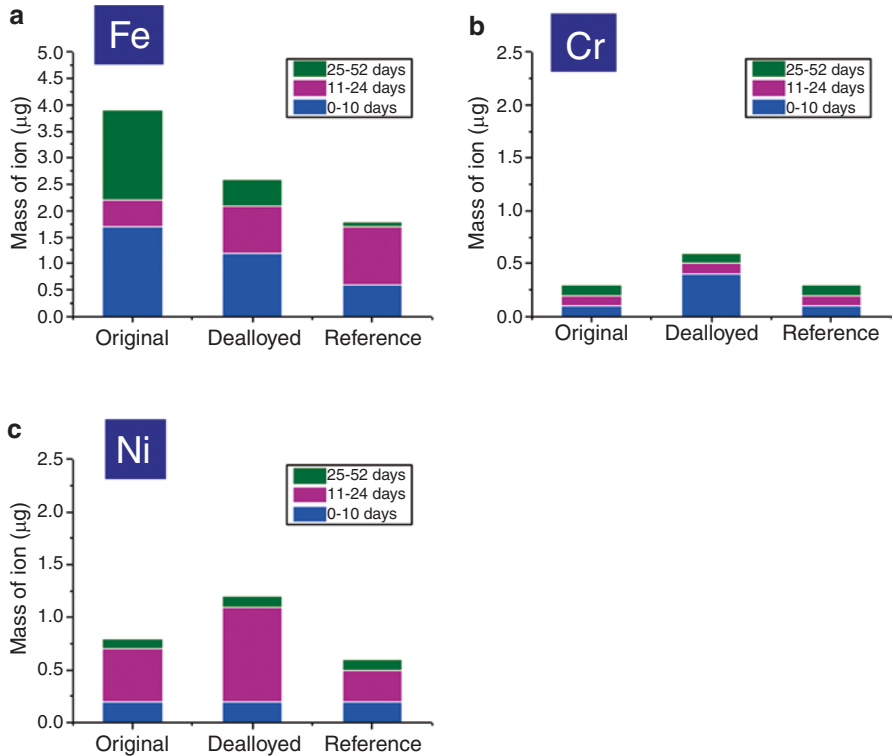


Fig. 3.13 Ion release of Fe (a), Cr (b), and Ni (c) from the surface of SUS316L dealloyed at 700 °C for 30 min compared with that of the original cold rolled SUS316L during the first 10 days (*blue*), 11–24 days (*pink*), and 25–52 days (*green*) immersion in HBSS. The HBSS was replaced with fresh solution after sampling at 10 and 24 days. Reference values are those measured with the same setup without the presence of a SUS316L sample

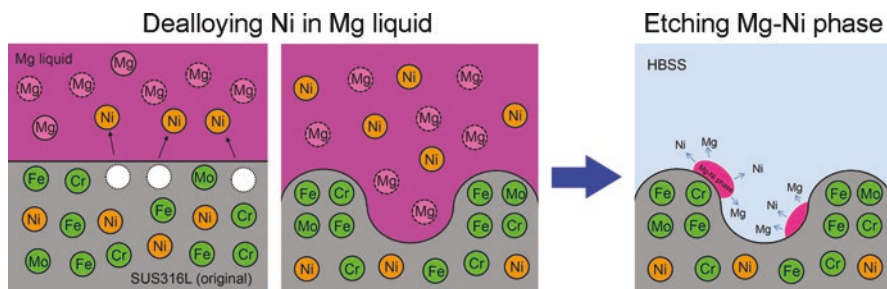


Fig. 3.14 Schematic illustration explaining origin of increased Ni ion release during 10–24 days immersion of the dealloyed SUS316L sample in HBSS. After dealloying treatment (*left*), Mg-Ni liquid solidified on the surface of the sample. Some Mg-Ni phase, perhaps located deep inside of the pores, remained even after the etching treatment in the aqueous HNO_3 solution (*right*). This phase likely dissolved slowly into the HBSS, resulting in a higher Ni ion release during this period

treatment, Ni-ion release could have been increased in the HBSS as shown in the following illustration (Fig. 3.14).

Dealloying tends to increase the surface area of the steel. This would increase the rate and amount of Ni ion release even after decreasing the concentration of Ni at the surface. If this is correct, then it should be possible to decrease the Ni ion release by decreasing the thickness of the reaction layer to decrease the surface area of treated steel.

3.4 Conclusions

1. The surface Ni concentration of SUS316L was successfully decreased from 11.8 to 2.2 at.% by dealloying the Ni in Mg liquid at 700 °C for 30 min.
2. Dealloyed SUS316L maintains excellent corrosion resistance in HBSS at room temperature.
3. Mass of Ni ion release from the Ni-dealloyed SUS316L surface was almost comparable or slightly increased compared with that of untreated SUS316L.
4. The main reasons for (3) are:
 - Increased surface area caused by the dealloying treatment, although the Ni concentration per unit area was decreased
 - Mg-Ni phase remaining on the sample surface after the etching in HNO_3 aqueous solution

Acknowledgment This research was financially supported by the interuniversity cooperative research program “Innovative Research for Biosis-Abiosis Intelligent Interface” from the Ministry of Sports, Culture, and Education of Japan.

References

1. Wada T, Yubuta K, Inoue A, Kato H. Dealloying by metallic melt. *Mater Lett.* 2011;65:1076–8. doi:[10.1016/j.matlet.2011.01.054](https://doi.org/10.1016/j.matlet.2011.01.054).
2. Fukuzumi Y, Wada T, Kato H. Surface improvement for biocompatibility of Ti-6Al-4V by dealloying in metallic melt. In: Sasaki K, Suzuki O, Takahashi N, editors. *Interface oral health science 2014. Innovative research on bionics-abiosis intelligent interface.* Springer Open; 2014. p. 93–101.
3. Forty AJ. Corrosion micromorphology of noble metal alloys and depletion gilding. *Nature.* 1979;282:597–8. doi:[10.1038/282597a0](https://doi.org/10.1038/282597a0).
4. Erlebacher J, Aziz MJ, Karma A, Dimitrov N, Sieradzki K. Evolution of nanoporosity in dealloying. *Nature.* 2001;410:450–3. doi:[10.1038/35068529](https://doi.org/10.1038/35068529).
5. Takeuchi A, Inoue A. Classification of bulk metallic glasses by atomic size difference, heat of mixing and period of constituent elements and its application to characterization of the main alloying element. *Mater Trans.* 2005;46:2817–29. doi:[10.2320/matertrans.46.2817](https://doi.org/10.2320/matertrans.46.2817).
6. Wada T, Setyawan AD, Yubuta K, Kato H. Nano- to submicro-porous β -Ti alloy prepared from dealloying in a metallic melt. *Scripta Mater.* 2011;65:532–5. doi:[10.1016/j.scriptamat.2011.06.019](https://doi.org/10.1016/j.scriptamat.2011.06.019).
7. Kim JW, Tsuda M, Wada T, Yubuta K, Kim SG, Kato H. Optimizing niobium dealloying with metallic melt to fabricate porous structure for electrolytic capacitors. *Acta Mater.* 2015;84:497–505. doi:[10.1016/j.actamat.2014.11.002](https://doi.org/10.1016/j.actamat.2014.11.002).
8. Wada T, Ichitsubo T, Yubuta K, Segawa H, Yoshida H, Kato H. Bulk-nanoporous-silicon negative electrode with extremely high cyclability for lithium-ion batteries prepared using a top-down process. *Nano Lett.* 2014;14:4505–10. doi:[10.1021/nl501500g](https://doi.org/10.1021/nl501500g).
9. Yu SG, Yubuta K, Wada T, Kato H. Three-dimensional bicontinuous porous graphite generated in low temperature metallic liquid. *Carbon.* 2016;96:403–10. doi:[10.1016/j.carbon.2015.09.093](https://doi.org/10.1016/j.carbon.2015.09.093).

Open Access This chapter is distributed under the terms of the Creative Commons Attribution 4.0 International License (<http://creativecommons.org/licenses/by/4.0/>), which permits use, duplication, adaptation, distribution and reproduction in any medium or format, as long as you give appropriate credit to the original author(s) and the source, provide a link to the Creative Commons license and indicate if changes were made.

The images or other third party material in this chapter are included in the work's Creative Commons license, unless indicated otherwise in the credit line; if such material is not included in the work's Creative Commons license and the respective action is not permitted by statutory regulation, users will need to obtain permission from the license holder to duplicate, adapt or reproduce the material.

